

# Shenqi Fuzheng Injection Reduces Cisplatin-Induced Kidney Injury via cGAS/STING Signaling Pathway in Breast Cancer Mice Model

Yingrui Ma<sup>1,\*</sup>, Bufan Bai<sup>1,\*</sup>, Deng Liu<sup>1</sup>, Rong Shi<sup>2</sup>, Qianmei Zhou<sup>1,3</sup> 

<sup>1</sup>Institute of Interdisciplinary Integrative Medicine Research, Shanghai University of Traditional Chinese Medicine, Shanghai, People's Republic of China;

<sup>2</sup>Department of Intensive Care Medicine, Shuguang Hospital Affiliated to Shanghai University of Traditional Chinese Medicine, Shanghai, People's Republic of China; <sup>3</sup>Shanghai Institute of Stem Cell Research and Clinical Translation, Dongfang Hospital Affiliated to Shanghai Tongji University, Shanghai, People's Republic of China

\*These authors contributed equally to this work

Correspondence: Rong Shi, Department of Intensive Care Medicine, Shuguang Hospital Affiliated to Shanghai University of Traditional Chinese Medicine Shanghai, Shanghai, People's Republic of China, Email doctorshi@126.com; Qianmei Zhou, Institute of Interdisciplinary Integrative Medicine Research, Shanghai University of Traditional Chinese Medicine, Shanghai, People's Republic of China, Email tazhou@163.com

**Background:** Shenqi Fuzheng Injection (SQFZ) is a traditional Chinese medicine injection consists of extracts of *Codonopsis pilosula* and *Astragalus mongholicus*. Combining SQFZ with conventional chemotherapy may improve the therapeutic efficacy and reduce side-effects of chemotherapy. However, the mechanisms of SQFZ reducing cisplatin-induced kidney injury are still unclear.

**Methods:** The main compounds of SQFZ were identified via UPLC-Q-TOF-MS technique. Using multiple databases to predict potential targets for SQFZ. We established a breast cancer model by injecting 4T1 cells into mice. Tumor growth and body weight were observed. Serum blood urea nitrogen (BUN), creatinine (CRE), and glutathione (GSH) levels were measured. The extent of their kidney injury was measured by hematoxylin-eosin staining (HE). Cell apoptosis was identified using Hoechst33258 staining, flow cytometry and TUNEL. We evaluated H2AX and stimulator of interferon genes (STING) expression by immunohistochemistry (IHC), and assessed apoptosis-associated proteins by Western blotting analysis. We also evaluated mitochondrial function. The secretion of the inflammatory cytokines in serum was observed using ELISA assay. The effect of the STING pathway in HK-2 renal tubular epithelial cells exposed to cisplatin alone or combined with SQFZ.

**Results:** The potential targets of SQFZ on kidney injury mainly related to inflammatory responses, oxidation and antioxidant, apoptosis as well as IFN signaling pathway. Cisplatin significantly reduced animal weight, while there were no changes in the combination SQFZ and cisplatin. SQFZ counteracted cisplatin-induced BUN and CRE elevation. SQFZ ameliorated the oxidative stress induced by cisplatin. It diminished cisplatin-induced apoptosis and mitochondrial DNA damage and reversed cisplatin-induced cyclic guanosine monophosphate-adenosine monophosphate synthase (cGAS)/STING signaling pathway activation. It also improved the mitochondrial dysfunction induced by cisplatin.

**Conclusions:** The results of the present study suggested that SQFZ effectively reduced cisplatin-induced kidney injury by inhibiting cGAS/STING signaling pathway.

**Keywords:** Shenqi Fuzheng Injection, cisplatin, kidney injury, mitochondrial, cGAS/STING, breast cancer, network pharmacology

## Introduction

Breast cancer is a serious threat to women's health. Breast cancer has the highest incidence rate and the second largest mortality rate after lung cancer among women in several countries.<sup>1-4</sup> Moreover, the incidence of breast cancer is predicted to increase.<sup>5,6</sup> Age, family history and obesity are all linked to breast cancer.<sup>7,8</sup> Common chemotherapeutic agents used for breast cancer include cyclophosphamide, doxorubicin, tamoxifen, paclitaxel, and cisplatin.<sup>9</sup> Cisplatin is effective as a chemotherapeutic agent that works primarily by eliciting a DNA damage response and can be used to against various solid tumors including breast cancer.<sup>10-12</sup> However, cisplatin chemotherapy is associated with severe adverse reactions and

may be nephrotoxic,<sup>13</sup> neurotoxic,<sup>14</sup> ototoxic,<sup>15</sup> hepatotoxic,<sup>16</sup> and cardiotoxic.<sup>17</sup> The nephrotoxicity of cisplatin has been widely investigated. This drug is a major cause of common clinical acute kidney injury (AKI).<sup>18,19</sup> Cisplatin-induced AKI (cAKI) affects mainly the renal tubular epithelial cells.<sup>20</sup> Ameliorating cAKI and attenuating the side effects of cisplatin chemotherapy are key clinical issues in cancer treatment and remain to be resolved.

The mechanism of cAKI is complex and comprises mitochondrial and DNA damage, oxidative stress, apoptosis, and inflammation.<sup>13</sup> Mitochondria are vital organelles in eukaryotic cells and regulate ATP production, cellular metabolism, redox homeostasis,<sup>21</sup> apoptosis, and necrosis. They initiate intrinsic apoptosis via mitochondrial outer membrane permeabilization (MOMP) and the latter is elicited by the pro-apoptotic Bcl2 family proteins Bax and Bak1.<sup>22</sup> Cisplatin caused Bax and Bak1 accumulation and oligomerization in mitochondria which resulted in renal tubular epithelial cell apoptosis. However, Bcl2 overexpression ameliorated cisplatin-induced apoptosis.<sup>23</sup> SQFZ has been found to inhibit the expression of anti-apoptotic Bcl2 in lung cancer.<sup>24</sup> Whether SQFZ has an effect on the ratio of Bax/Bcl2 in renal tubular epithelial cell is worth exploring. Mitochondria are abundant in renal tubular epithelial cells, and mitochondrial dysfunction is an integral part of the development of renal injury.<sup>21</sup> For these reasons, maintaining mitochondrial homeostasis is essential for normal kidney function.

In a healthy body, the oxidant and antioxidant levels are in equilibrium. However, when this balance is disrupted, oxidative stress occurs, which is one of the mechanisms of cisplatin induced kidney injury.<sup>25</sup> Mitochondria may be important sources of intracellular reactive oxygen species (ROS).<sup>26</sup> They produce excessive ROS in response to cisplatin-mediated injury, attenuate or downregulate antioxidants such as glutathione (GSH), superoxide dismutase (SOD), and catalase, and exacerbate existing mitochondrial damage.<sup>27,28</sup> Excessive ROS production and accumulation caused renal tubular epithelial cell apoptosis in mice.<sup>29,30</sup>

Cisplatin elicits a DNA damage response (DDR) by inhibiting DNA replication and transcription.<sup>31</sup> Mitochondrial DNA (mtDNA) is relatively more susceptible to oxidative stress than nuclear double-stranded (ds) DNA. Cisplatin-induced oxidative stress may damage mtDNA, cause mitochondrial dysfunction, and aggravate kidney injury already present.<sup>32,33</sup> Oxidative stress activates the cyclic guanosine monophosphate (GMP)-adenosine monophosphate (AMP) synthase (cGAS) and stimulator of interferon genes (STING) (cGAS-STING) signaling pathways.<sup>34</sup> The cGAS-STING signaling pathway senses innate immune responses and is activated in cAKI.<sup>35</sup> Both dsDNA and mtDNA activate the cGAS-STING signaling pathway. As cisplatin disrupts the mitochondria in renal tubular epithelial cells, it causes mtDNA to leak into the cytoplasm. In response, the cGAS-STING signaling pathway is activated, inflammation occurs, and kidney injury is worsened.<sup>36</sup> It has been shown that maintaining mitochondrial homeostasis can prevent DNA leakage and exert anti-tumor effects.<sup>37,38</sup> Based on the downstream signaling pathways that can be activated by DNA to affect the occurrence and development of tumors, the latest research has demonstrated the use of ultra-sensitive DNA origami plasmonic sensors for precise detection of circulating tumor DNA (ctDNA), providing a new tool for early diagnosis and treatment decision-making of lung cancer.<sup>39</sup> Our research on DNA damage can further reveal the mechanism of alleviating the side effects of cisplatin and enhancing its anti-tumor effect.

Several studies showed that Shenqi Fuzheng Injection (SQFZ) can alleviate the adverse reactions associated with cancer chemotherapy.<sup>40</sup> SQFZ consists of extracts of *Codonopsis Radix* (CR) and *Astragali Radix* (AR).<sup>41</sup> CR has the effect of nourishing the middle and qi, while AR can enhance yang and qi.<sup>42,43</sup> The combination of the two drugs can supplement the center and boost qi, achieving the effect of supporting the body's positive energy to fight against cancer.<sup>44,45</sup> Therefore, SQFZ can alleviate the toxic effects of chemotherapy while improving its therapeutic efficacy.<sup>46-49</sup>

In an earlier study, we demonstrated that SQFZ reversed M2 macrophage-mediated cisplatin resistance in breast cancer via the phosphoinositide 3-kinase (PI3K) signaling pathway.<sup>50</sup> We also discovered that SQFZ attenuated cisplatin toxicity in breast cancer treatment. However, we have not yet elucidated the underlying mechanisms involved. The present study aimed to link mitochondrial function with the putative efficacy of SQFZ against cisplatin-induced nephrotoxicity.

## Materials and Methods

### UPLC-Q-TOF-MS

The samples of SQFZ were analyzed by ultra-high performance liquid chromatography-high-resolution mass spectrometry (UPLC-Q-TOF-MS). The main compounds of SQFZ were identified according to the multistage mass spectrometry

information of the samples, combined with the high-resolution mass spectrometry database of natural products and related literature. The data acquisition software was Analyst TF1.7.1, and the data processing software was Peakview1.2. During identification, mass spectrometry data were first matched with Natural Products HR-MS/MS Spectral Library 1.0 database.

## Network Pharmacology

### Potential Targets of Main Components of SQFZ

According to the mass spectrometry results, based on TCMSp ([https://tcmsp-e.com/load\\_intro.php?id=29](https://tcmsp-e.com/load_intro.php?id=29)), HERB (<http://herb.ac.cn/Detail/?v=HBIN026630&label=Ingredient>), HIT (<http://hit2.badd-cao.net/>), PubChem (<https://pubchem.ncbi.nlm.nih.gov/>), Swiss Target Prediction Database (<http://www.swisstargetprediction.ch/>) to retrieve main ingredients of potential target point. Use the UniProt (<https://www.uniprot.org/>), STRING ([https://string-db.org/cgi/input?sessionId=bWts2URU97qvandinput\\_page\\_show\\_search=on](https://string-db.org/cgi/input?sessionId=bWts2URU97qvandinput_page_show_search=on)), the potential targets of SQFZ were screened and sorted in a unified format.

### Potential Targets of Kidney Injury

Based on online Mendelian genetic database (OMIM, <https://omim.org/>), the genome database (GeneCards, <https://www.genecards.org/>) and therapeutic targets database (TDD, <http://db.idrblab.net/ttd/>), the potential targets of “kidney injury” were observed. Venny (<https://bioinfogp.cnb.csic.es/tools/venny/>) was used to observe the intersection targets of SQFZ and kidney injury.

### Protein-Protein Interaction Network (PPI) Analysis of Potential Targets of SQFZ for Kidney Injury

The common potential targets of SQFZ and kidney injury were imported into the STRING platform (<https://string-db.org/>), and the protein species was set as “Homo sapiens”, the lowest interaction threshold was set as “medium confidence”. The protein interaction network data of potential targets were obtained. Then, the preliminary network topology analysis was carried out on Cytoscape 3.9.1 software. Based on the Average Shortest Path Length, Betweenness Centrality and other nodal topological indexes, the key targets of SQFZ in the treatment of kidney injury were obtained.

### KEGG Analysis on Key Targets

Using ClusterProfiler, Gene Ontology (GO) and Kyoto Encyclopedia of Gene and Genome (KEGG) enrichment analysis were performed under the condition of  $P < 0.05$ , and relevant histograms were drawn to explore the key signaling pathways and related protein enrichment of SQFZ in the treatment of kidney injury.

## Cell Culture and Treatment

Mouse breast cancer cell line (4T1) and renal tubular epithelial cell line (HK-2) were purchased from Shanghai Fuheng Biotechnology (Shanghai, China). The 4T1 cells were revived in high-glucose Dulbecco's modified Eagle's medium (DMEM) supplemented with 10% (v/v) fetal bovine serum (FBS). The HK-2 cell lines were revived in DMEM/F12 supplemented with 10% (v/v) FBS. Both cell lines were cultured under 5% CO<sub>2</sub> and at 37 °C. The HK-2 cells were loaded into 96-well and six-well plates. The next day, the cells were separated into treatment groups and incubated in various drug-containing media for 24 h. The treatments included 50 mL/L SQFZ, 10 μM cisplatin, 20 μM cisplatin, 80 μM cisplatin, 50 mL/L SQFZ + 10 μM cisplatin, 50 mL/L SQFZ + 20 μM cisplatin, and 50 mL/L SQFZ + 80 μM cisplatin. SQFZ (pharmaceutical factory batch No. 180820) was obtained from Lizhu Group Limin Pharmaceutical Co. Ltd. (Guangdong, China).

## Tumor Growth and Treatment

Female BALB/c mice aged 7 weeks were obtained from Vital River Laboratory Animal Technology (Shanghai, China). The 4T1 cells were resuspended in serum-free medium and injected into the mouse breast fat pads. Palpable tumors appeared after ~1 week and then the mice were randomly divided into the Control (n=7), 40 mL/kg SQFZ (n=9), 80 mL/kg SQFZ (n=9), 40 mL/kg SQFZ + 2 mg/kg cisplatin (n=9), 80 mL/kg SQFZ + 2 mg/kg cisplatin (n=9), and 2 mg/kg cisplatin (n=9) groups. Healthy uninoculated mice served as the Normal (n=7). All mice were injected daily with

physiological saline. The SQFZ and cisplatin were injected daily and every 3 d, respectively. Tumor size was determined every 3 d by vernier calipers, and tumor volume was calculated as shown in Eq. (1) below:

$$V(\text{mm}^3) = L(\text{major axis}) \times W^2(\text{minor axis}) / 2(1)$$

After 18 d treatment, blood was collected from the eyes of the mice, the animals were sacrificed by neck dislocation, and their tumors and kidney tissues were excised. The blood stood at room temperature (20–25 °C) for 1 h and was then centrifuged at 1200 g 4 °C for 15 min to collect the supernatants. All experimental procedures complied with animal welfare guidelines and were approved by the Ethics Committee of Shanghai Traditional Chinese Medicine under Approval No. PZSHUTCM220919006.

## Histological Examination

The kidney tissues were fixed in 4% (v/v) paraformaldehyde (PFA), embedded in paraffin, cut into 5- $\mu\text{m}$  sections (CM3050 S, Leica, Wetzlar, Germany), stained with hematoxylin-eosin (HE), and visualized under an optical microscope (IX73, Olympus, Tokyo, Japan).

## 3-(4,5-Dimethylthiazol-2-Yl)-2,5-Diphenyl-2H-Tetrazolium Bromide (MTT) Assay

The HK-2 cells were loaded into 96-well plates and exposed to various drug-containing cell culture media for 24 h. Cell viability was assessed by the MTT assay (Beyotime, Nanjing, China) according to the manufacturer's instructions. Cytotoxicity was determined based on the proportions of surviving cells as shown in Eq. (2) below:

$$\text{OD}_{\text{sample}} / \text{OD}_{\text{control}} \times 100\%(2)$$

## Blood Urea Nitrogen (BUN), Creatinine (CRE), and Glutathione (GSH) Measurements

The serum BUN, CRE, and GSH levels were separately determined with a multimode microplate reader according to the manufacturer's instructions (Nanjing Jiancheng Bioengineering Institute, Nanjing, China).

## Mitochondrial Reactive Oxygen Species (ROS) and Mitochondrial Membrane Potential ( $\Delta\psi\text{m}$ ; MMP) Assessments

The HK-2 cells were loaded into six-well plates, exposed to various drug concentrations for 24 h, collected, and subjected to probes (Beyotime, Nanjing, China) according to the manufacturer's instructions. ROS generation was evaluated with dichlorodihydrofluorescein diacetate (DCFH-DA) and Rosup served as a positive control. The probes were loaded and incubated at 37 °C for 30 min and analyzed in a multimode fluorescence microplate reader (Thermo Fisher Scientific, Waltham, MA, USA).  $\Delta\psi\text{m}$  was determined using JC-1 probes that were loaded and incubated at 37 °C for 30 min and detected in a multimode fluorescence microplate reader.  $\Delta\psi\text{m}$  was expressed in terms of the JC-1 monomer/JC-1 aggregate ratio.

## Terminal Deoxynucleotidyl Transferase-Mediated dUTP Nick-End Labeling (TUNEL) Staining

Kidney tissue sections were deparaffinized, treated with proteinase K, and incubated at 37 °C for 20 min. The TUNEL reaction mixture was then added and incubated in the dark at 37 °C for 60 min. Then 4',6-diamidino-2-phenylindole (DAPI) nuclear stain was added, the mixture was incubated at room temperature (20–25 °C) for 10 min, and the sections were observed under a fluorescence microscope and photographed (IX73, 200 x, Olympus, Tokyo, Japan).

## Hoechst 33258 Staining

The HK-2 cells were loaded into six-well plates and subjected to various drug-containing media for 24 h. The cells then underwent Hoechst 33258 staining according to the manufacturer's instructions, were incubated at 37 °C for 30 min, and were observed under a fluorescence microscope and photographed (IX73, 100 x, Olympus, Tokyo, Japan).

## Flow Cytometry

The HK-2 cells were loaded into six-well plates, subjected to various drug-containing media for 24 h, and double-stained with Annexin V-FITC and propidium iodide (PI) according to the manufacturer's protocol (Beyotime, Nanjing, China). The data were collected with a fluorescence activating cell sorter (FACS) (CytoFLEX, Beckman Coulter, Brea, CA, USA) and analyzed with CytExpert (Beckman Coulter).

## Immunohistochemical (IHC) Assay

IHC was used to detect H2A.X and STING expression in the mouse kidney specimens. The sections were deparaffinized and dehydrated in an ethanol gradient, immersed in 0.01 M citrate buffer (pH 6.0), microwaved for 10 min, incubated in deionized water with 3% H<sub>2</sub>O<sub>2</sub> at room temperature (20–25 °C) for 10 min, and rinsed thrice with phosphate-buffered saline (PBS) for 3 min each time. The PBS was then removed and replaced with non-immune serum and the sections were incubated at room temperature (20–25 °C) for 10 min. Primary antibodies (anti-Histone H2A.X, anti-STING) were then added and the sections were incubated at 4 °C overnight and rinsed thrice with PBS for 3 min each time. Secondary antibodies (anti-Rabbit IgG, #A10040, 1:1,000, Thermo Fisher Scientific) were then sequentially added to the sections and the latter were incubated at room temperature (20–25 °C) for 10 min and rinsed thrice with PBS for 3 min each time. Then 3,3'-diaminobenzidine (DAB) color development solution was added to the sections. The latter were then subjected to hematoxylin re-staining, ethanol gradient dehydration, drying, and sealing. The nuclei were then stained with DAPI. The anti-Histone H2A.X (#7631, 1:100) and anti-STING (#13647, 1:100) monoclonal antibodies were purchased from Cell Signaling Technology (CST), Danvers, MA, USA.

## Western Blot Analysis

A mixture of lysate and protease inhibitor was added to the cells and their total protein was extracted. The protein was quantified with a bicinchoninic acid (BCA) reagent kit (Beyotime, Nanjing, China). Loading buffer was added to the mixture and the latter was then boiled to denature the protein therein. The mixture was then subjected to sodium dodecyl sulfate-polyacrylamide gel electrophoresis (SDS-PAGE) and transferred onto a polyvinylidene difluoride (PVDF) membrane. The latter was blocked with bovine serum albumin (BSA) for 1 h, primary antibody (1:1,000) was added to it, and the membrane was incubated 6 h. Then secondary antibody (1:1,000) was added and the membrane was incubated at room temperature (20–25 °C) for 2 h. The membrane was then exposed to immobilon western chemiluminescence horseradish peroxidase (HRP) substrate and the protein bands were detected by luminescence imaging (Tanon, Shanghai, China). The Western blots were quantified with ImageJ (National Institute of Health [NIH], Bethesda, MD, USA). The anti-H2A.X, anti-cGAS, anti-STING, anti-Bax, and anti-Bcl2 monoclonal antibodies were purchased from CST.

## ATP Measurement

HK-2 cells were loaded into six-well plates and subjected to various drug-containing media for 24 h. Their ATP levels were measured with an ATP Assay Kit (Beyotime, Nanjing, China) according to the manufacturer's instructions. The cell lysis supernatants and ATP assay solutions were loaded into a white 96-well plate and their fluorescence was measured with a multimode fluorescence microplate reader (Thermo Fisher Scientific). The ATP levels were expressed as nmol/mg protein.

## RNA Extraction and Quantitative Real-Time PCR

Extract RNA according to the instructions of the UNIQ-10 column Trizol total RNA extraction kit, and performed RNA concentration and quality testing according to the instructions of the One Step RT-qPCR Kit (dye method) kit (Sangon Biotech). Relative gene expression levels were calculated with the comparative cycle threshold (CT;  $2^{-\Delta\Delta Ct}$ ) method. Primer sequences are listed:

IL-6 Forward- TTCGGTCCAGTTGCCTTCTCC, Reverse- TCTGAAGAGGTGAGTGGCTGTC; IL-8 Forward- CTCTTGGCAGCCTTCCTGATTTC, Reverse- GGGTGGAAAGGTTTGGAGTATGTC; CCL5 Forward- CGCTGTCATC

CTCATTGCTACTG, Reverse- GCCACTGGTGTAGAAATACTCCTTG; NO Forward- TCATTCTGTCCGTCTCT TCAA, Reverse- ATCAGATCTGAGATGATCACCG.

## RNA Interference

The expression of STING was suppressed with a siRNA (si-STING1 sense: CCCGGAUUCGAACUUACAATT, si-STING1 antisense: UUGUAAGUUCGAAUCCGGGCC). Results were compared with a control siRNA. The siRNAs were transfected into HK-2 cells using Lipofectamine RNAiMAX transfection reagent (Thermo Fisher Scientific).

## Enzyme Linked Immunosorbent (ELISA) Assay

Serum was harvested and quantified by the Bradford method (Bio-Rad, Hercules, CA; n = 6 per group). The levels of IL-6, IL-8, CCL5 and NO were quantified using an ELISA kit according to the manufacturer's directions (eBioscience, San Diego, CA).

## Statistical Analysis

Data was means  $\pm$  standard deviation (SD). Student's *t*-test was run to identify differences between group pairs. One-way ANOVA was run to identify differences among  $\geq$  three groups. Differences were considered significant at  $P < 0.05$ .

## Results

### Identification of Main Components and Target Prediction of SQFZ

Based on UPLC-Q-TOF-MS, multistage mass spectrometry information of samples, high-resolution mass spectrometry database of natural products and related literatures, 20 main compounds were identified from SQFZ ([Supplemental Figure 1](#)).

By integrating the obtained targets through STRING and UniProt databases, 282 potential targets for SQFZ were selected. OMIM, GeneCards and TTD databases were used to find 816 potential target genes of kidney injury. Finally, 65 potential targets of SQFZ were found for the treatment of kidney injury ([Supplemental Table 1](#)), and obtained the Venn diagram showing the correlation between SQFZ and kidney injury ([Figure 1A](#)).

The PPI network based on the common potential targets of SQFZ and kidney injury showed that there were 65 nodes and 894 edges ([Figure 1B](#)). Kidney injury, main ingredients of SQFZ and 65 selected important targets were integrated and analyzed by Cytoscape software to generate the network between SQFZ and kidney injury ([Figure 1C](#)). It showed that there were multiple interaction relationships between SQFZ and kidney injury. The associated potential genes were Bax, Bcl2, oxidative stress, inflammatory mediators and IFNG. The main compounds of SQFZ were Astragaloside IV, Azelaic Acid, Calycosin 7-O-glucoside, Cyclocephaloside II, Guanosine, Lobetyolin, Markhamioside F, Methylnissolin-3-O-glucoside and Saccharumoside C.

The top enrichment targets for BP, CC and MF were shown in [Figure 1D](#). It showed 20 related functions and pathways with high enrichment. These included proteoglycan in cancer, microRNAs in cancer, phosphatidylinositol 3-kinase/protein kinase B (PI3K/Akt) signaling pathway, breast cancer, T cell receptor signaling pathway, hypoxia Inducing-factor-1 (HIF1) signaling pathway ([Figure 1E](#)). Therefore, we explored the mechanisms of SQFZ in alleviating cisplatin-induced nephrotoxicity through cell apoptosis, oxidative stress, and interferon pathways.

### Shenqi Fuzheng Injection Alleviated Cisplatin-Induced Kidney Injury

The chemotherapeutic agent cisplatin is commonly administered in clinical practice. However, it may cause severe kidney injury.<sup>18</sup> Therefore, this adverse reaction must be mitigated to enhance the therapeutic efficacy of cisplatin. We inoculated BALB/c mice with 4T1 cells to establish a mouse breast cancer model and determine the role of SQFZ in the amelioration of cisplatin-induced renal injury during breast cancer treatment. Three days after model induction, we intraperitoneally (IP) injected SQFZ (40 or 80 mL/kg) and cisplatin (2 mg/kg) for 18 d. The tumor volumes of the mice treated with 40 mL/kg SQFZ, 80 mL/kg SQFZ, and 2 mg/kg cisplatin were 15.58%, 16.47%, and 24.63% smaller, respectively than those of the untreated control mice. However, the tumor volumes of the mice treated with a combination of 40 mL/kg SQFZ plus 2 mg/kg cisplatin and those treated with 80 mL/kg plus 2 mg/kg cisplatin

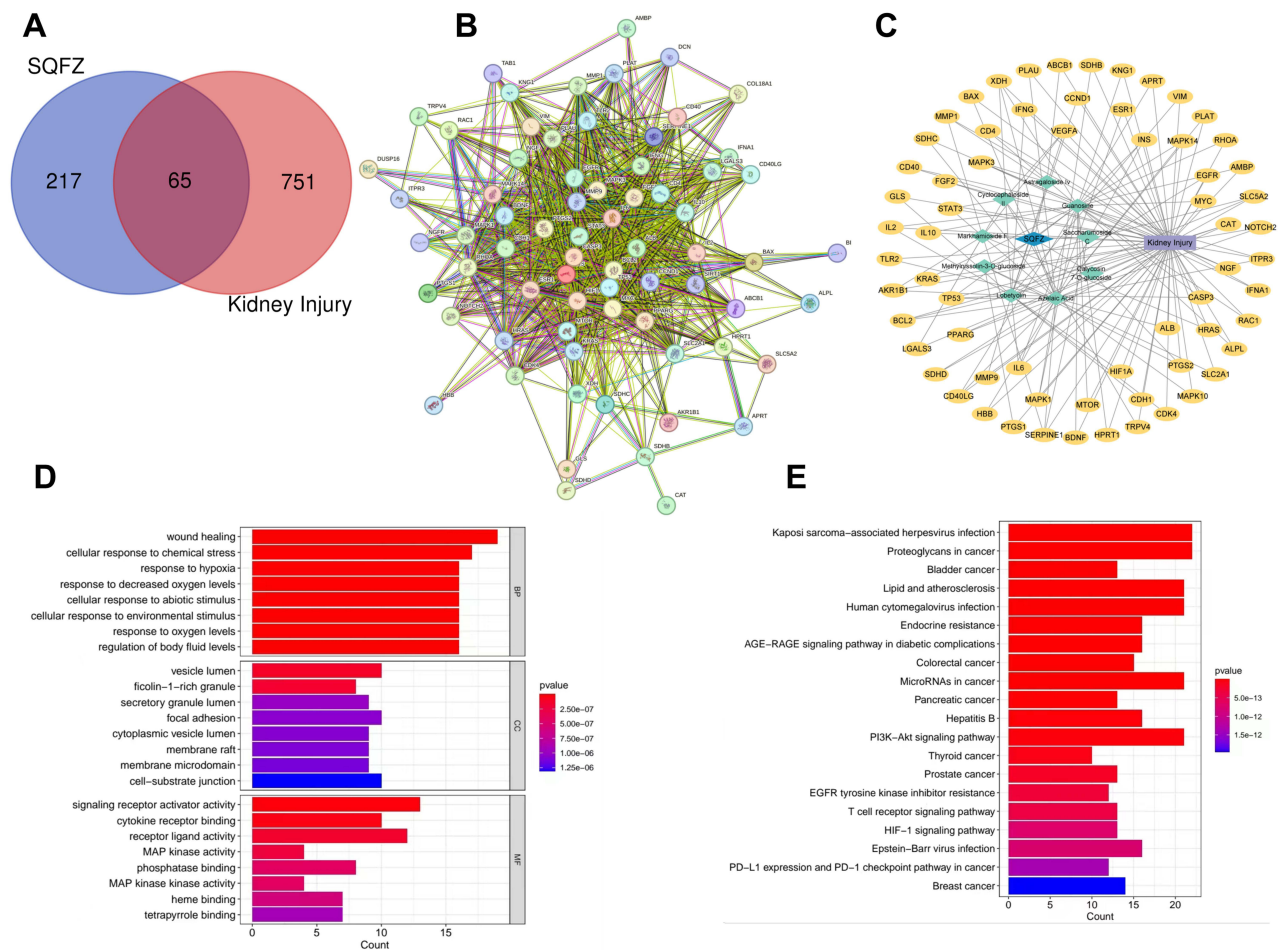


**Figure 1** Prediction of potential targets for Shenqi Fuzheng injection and kidney injury. **(A)** Venn Diagram of main components of Shenqi Fuzheng injection and kidney injury. **(B)** Shenqi Fuzheng injection - kidney injury protein-protein interaction network (PPI). **(C)** The main targets network of Shenqi Fuzheng injection and kidney injury. **(D)** Gene ontology (GO) analysis (Histogram). **(E)** Kyoto Encyclopedia of Genes and Genomes (KEGG) Analysis (Histogram).

were 42.75% and 59.63% smaller, respectively than those of the untreated control mice ( $P < 0.05$ ). These findings suggest that SQFZ significantly enhanced the tumor-shrinking efficacy of cisplatin (Figure 2A and B). Compared to the untreated control, the cisplatin treatment lowered the body weight by 34.82% but the 40 mL/kg and 80 mL/kg SQFZ treatments did not significantly change it. However, the combinations of 40 mL/kg plus 2 mg/kg cisplatin and 80 mL/kg SQFZ plus 2 mg/kg cisplatin lowered the body weight by 26.15% and 24.08%, respectively relative to the untreated control ( $P < 0.05$ ) (Figure 2C).

Serum blood urea nitrogen (BUN) and creatinine (CRE) are important renal function indices. Here, cisplatin alone dramatically upregulated BUN and CRE whereas the combination of 40 mL/kg SQFZ plus cisplatin and especially 80 mL/kg SQFZ plus cisplatin significantly reversed these changes (Figure 2D and E). The serum BUN levels following the 40 mL/kg SQFZ plus cisplatin and 80 mL/kg SQFZ plus cisplatin treatments were 24.02% and 28.84% lower, respectively than that following the cisplatin treatment alone. The serum CRE levels following the 40 mL/kg SQFZ plus cisplatin and 80 mL/kg SQFZ plus cisplatin treatments were 26.73% and 36.63% lower, respectively than those following the cisplatin treatment alone ( $P < 0.05$ ).

Hematoxylin-eosin staining (HE) showed that the mice subjected to cisplatin alone presented renal tubular injury characterized by renal tubular epithelial cell vacuolation, swelling, and necrosis. However, renal tubular injury was significantly less severe in response to the SQFZ-cisplatin combinations than cisplatin alone (Figure 2F).

We performed in vitro proliferation assays on renal tubular epithelial cells HK-2 to demonstrate the protective effect of SQFZ. Figure 2G showed that SQFZ alone had no negative effect on HK-2 cell proliferation even at high

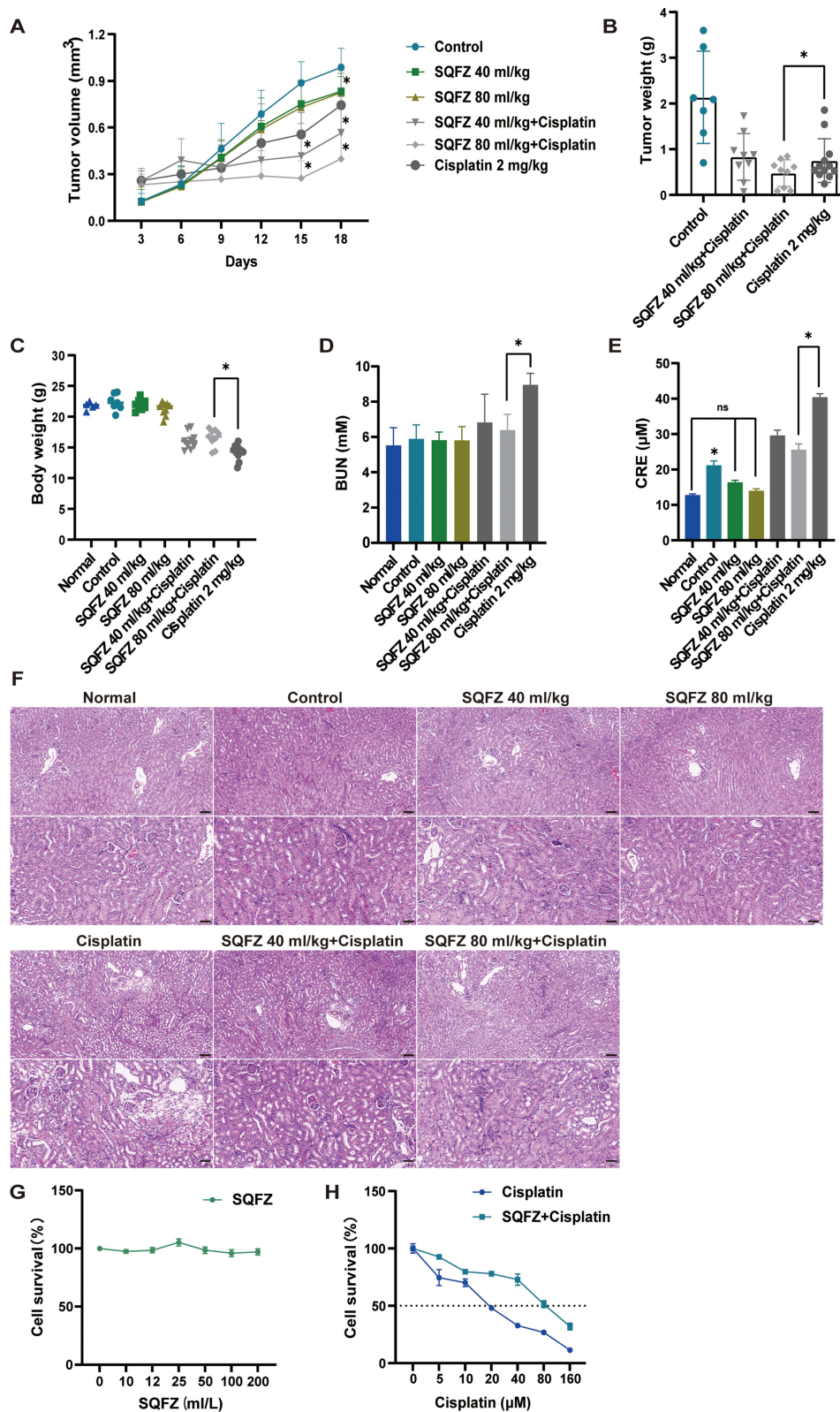


**Figure 2** Cisplatin-induced kidney injury was alleviated by Shenqi Fuzheng injection. (A-F) BALB/c mice inoculated with 4T1 cells in the fat pads were treated with daily intraperitoneal injections of saline or SQZ 40, 80 mL/kg, cisplatin 2 mg/kg, SQZ 40 mL/kg + cisplatin (injected every three days), and SQZ 80 mL/kg + cisplatin (injected every three days) for 18 days. (A) Dynamic recording of tumor volume in mice. Calculation of Tumor Volume:  $V \text{ (mm}^3\text{)} = L \text{ (major axis)} \times W^2 \text{ (minor axis)}/2$ . (B and C) Final weight of tumors and body weight of mice. (D and E) BUN and CRE levels in the serum of mice. (F) H&E staining of mouse kidney. (Scale bar = 100 μm, 50 μm) (G) HK-2 cells were cultured in SQZ at 0, 10, 12, 25, 50, 100, 200 mL/L for 24 h. Cell viability was assessed using MTT assay. (H) HK-2 cells were cultured in cisplatin at 0, 5, 10, 20, 40, 80, 160 mL/L or cisplatin combined with SQZ (50 mL/L) for 24 h. Cell viability was assessed using MTT assay. Data are presented as mean ± SD. ns, not significant. \* $P < 0.05$  as compared to Cisplatin alone.

concentrations. Figure 2H showed the protective efficacy of SQFZ against cisplatin-induced renal injury. Cisplatin markedly inhibited HK-2 cell proliferation ( $IC_{50} = 20.17 \mu\text{M}$ ) whereas SQFZ significantly reversed this inhibition ( $IC_{50} = 70.84 \mu\text{M}$ ).

## Shenqi Fuzheng Injection Improved Oxidative Damage in vitro and in vivo

Oxidative stress injury is an important indicator of cisplatin-induced renal injury.<sup>26</sup> Disruption of the redox balance led to reactive oxygen species (ROS) accumulation which, in turn, caused mitochondrial dysfunction.<sup>51</sup> The antioxidant glutathione (GSH) cleared intracellular ROS and mitigated the intracellular damage caused by oxidative stress.<sup>52</sup> In the mice, cisplatin alone downregulated GSH by 73.16% relative to the untreated control whereas 40 mL/kg SQFZ plus cisplatin and 80 mL/kg SQFZ plus cisplatin significantly reversed GSH reduction ( $P < 0.05$ ) (Figure 3A). We measured the ROS levels in HK-2 cells to investigate the relationship between oxidative stress and kidney injury in vitro. Cisplatin alone substantially increased the ROS levels compared with the untreated control. The ROS level was positively correlated with the cisplatin concentration. In the cells subjected to 80  $\mu\text{M}$  cisplatin, the ROS level was 1.99-fold higher than that in the untreated control. Nevertheless, SQFZ addition reversed these changes ( $P < 0.05$ ) (Figure 3B).

## Shenqi Fuzheng Injection Reduced Cisplatin-Induced Apoptosis in vitro and in vivo

We then measured terminal deoxynucleotidyl transferase-mediated dUTP nick end labeling (TUNEL) staining in mouse kidneys and Hoechst 33258 staining in HK-2 cells to determine the roles of SQFZ in cisplatin-induced apoptosis in vitro and in vivo. The TUNEL staining revealed that the renal tubular epithelial cells of the mice treated with 40 mL/kg SQFZ plus cisplatin or 80 mL/kg SQFZ plus cisplatin exhibited less apoptosis than those of the mice treated with cisplatin alone (Figure 4A). The Hoechst 33258 staining disclosed that the HK-2 cells exposed to SQFZ plus cisplatin presented significantly fewer fragmented, densely stained nuclei than those treated with cisplatin alone (Figure 4B). We also stained HK-2 cells with Annexin V-FITC and propidium iodide (PI) and used flow cytometry to detect apoptosis. The Annexin V-FITC assay showed that treatment with 10  $\mu\text{M}$ , 20  $\mu\text{M}$ , or 80  $\mu\text{M}$  cisplatin significantly increased the number of apoptotic and necrotic cells relative to the untreated control. However, the combined SQFZ-cisplatin treatments reversed these effects to a certain degree (Figure 4C). Compared to the 80  $\mu\text{M}$  cisplatin treatment, the combined SQFZ-cisplatin treatment reduced apoptosis and necrosis from 75.87% to 54.76%.

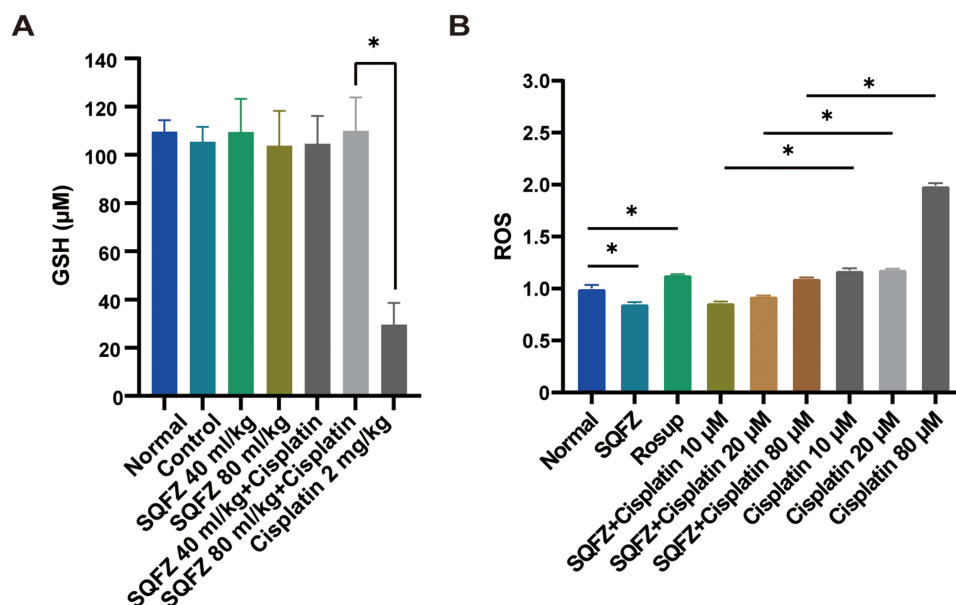


**Figure 3** Shenqi Fuzheng Injection improved oxidative damage in vivo and in vitro. (A) GSH levels in the serum of mice. (B) Results of ROS assay in HK-2 cells after SQFZ and cisplatin treatment for 24 h. Data are presented as mean  $\pm$  SD. ns, not significant. \* $P < 0.05$  as compared to Cisplatin alone.

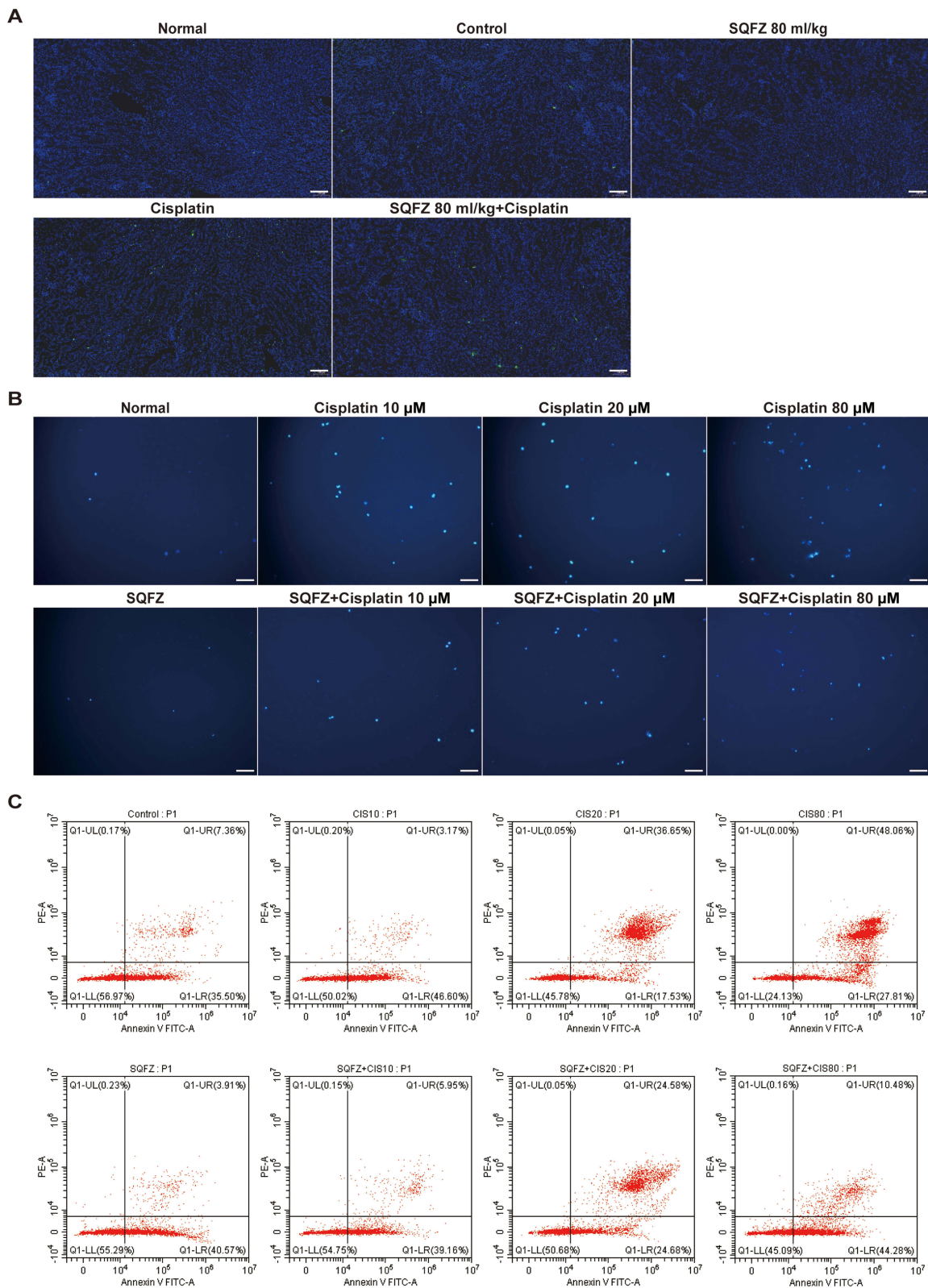


**Figure 4** Shenqi Fuzheng Injection reduced cisplatin-induced apoptosis in vitro and in vivo. **(A)** TUNEL staining results of mouse kidney tissues in each treatment group. (Scale bar =100 μm) **(B)** HK-2 cells were treated with SQZ and cisplatin for 24 h and then stained using Hoechst 33258 and photographed by fluorescence microscopy. (Magnification: 100 ×) **(C)** HK-2 cells SQZ and cisplatin treated for 24 h were tested using flow cytometry analysis of apoptosis based on Annexin V-FITC/PI. **Abbreviation** CIS, Cisplatin.

**Shenqi Fuzheng Injection Mitigated Cisplatin-Induced DNA Damage in vitro and in vivo**

DNA damage is associated with cisplatin-induced kidney injury. The histone H2A variant H2A.X is phosphorylated at Ser 139 (H2A.X) and may be used to detect DNA damage.<sup>53</sup> We evaluated H2A.X expression to examine the effects of SQFZ on cisplatin-induced DNA damage in renal tubular epithelial cells. An immunohistochemical (IHC) analysis of mouse kidney tissues showed that while the cisplatin treatment strongly upregulated H2A.X, the 40 mL/kg SQFZ plus cisplatin and the 80 mL/kg SQFZ plus cisplatin treatments only slightly increased H2A.X expression (Figure 5A). The SQFZ treatment alone did not affect H2A.X expression. Western blotting showed that H2A.X expression had significantly increased in HK-2 cells exposed to 80  $\mu$ M cisplatin for 24 h while the combined SQFZ plus cisplatin treatment reversed this trend (Figure 5B and C). Whereas 10  $\mu$ M and 20  $\mu$ M cisplatin alone did not upregulate H2A.X, the SQFZ plus 10  $\mu$ M cisplatin and SQFZ plus 20  $\mu$ M cisplatin treatments downregulated H2A.X in the HK-2 cells ( $P < 0.05$ ).

### Shenqi Fuzheng Injection regulated the cGAS/STING signaling pathway in cisplatin-treated mouse kidney and HK-2 cells

Acute kidney injury is associated with mitochondrial damage, mitochondrial DNA (mtDNA) leakage into the cytosol, cGAS/STING signaling pathway activation, and tubular inflammation.<sup>36</sup> We measured the expression levels of cGAS/STING-related proteins in mouse kidney and HK-2 cells to determine the modes of action of SQFZ in cisplatin-induced renal injury. The mouse kidney IHC analysis indicated that STING was significantly upregulated in response to cisplatin alone but was downregulated following the 40 mL/kg SQFZ plus cisplatin and the 80 mL/kg SQFZ plus cisplatin treatments (Figure 6A). Moreover, the cGAS

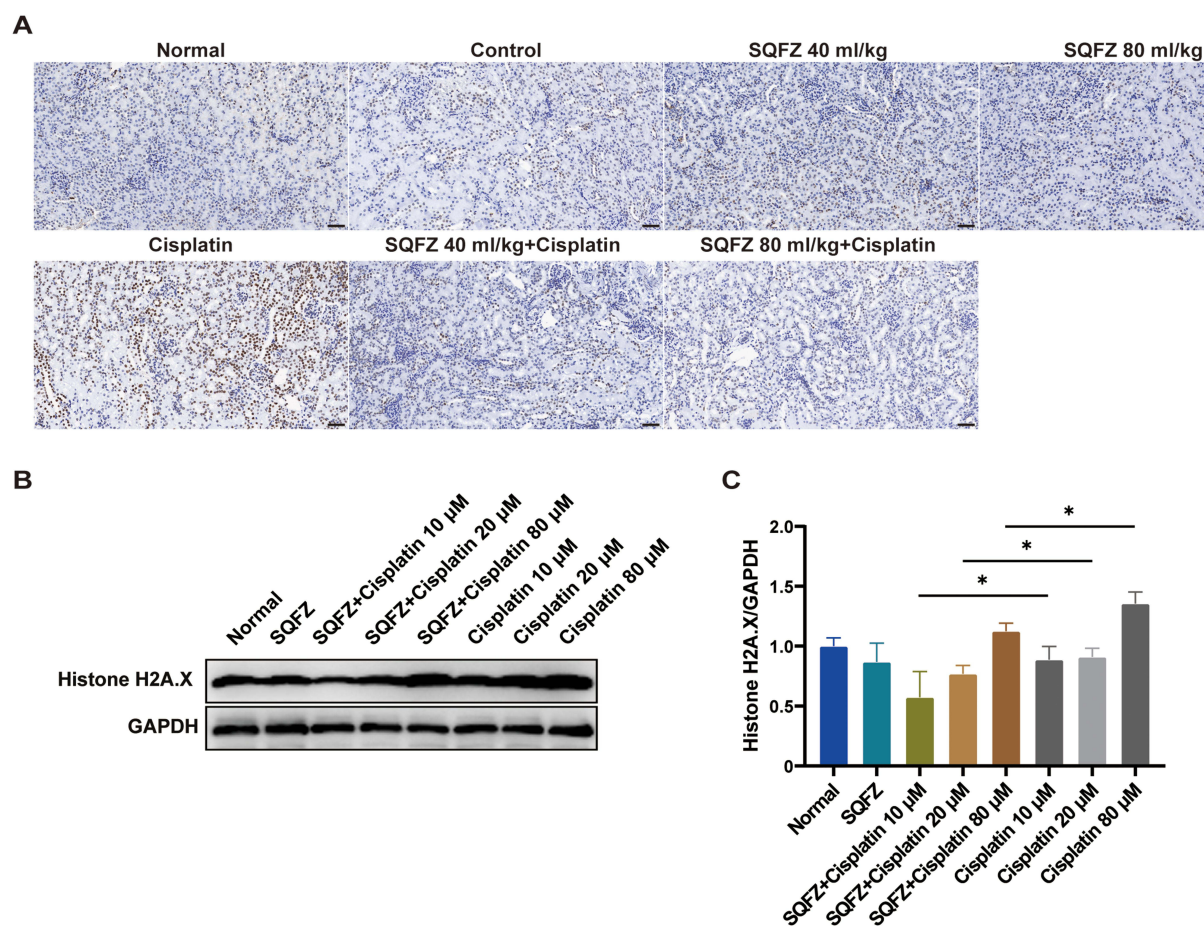


**Figure 5** Shenqi Fuzheng Injection decreased cisplatin-induced DNA damage in vitro and in vivo. (A) Immunohistochemical results of H2AX in kidney tissues of mice in each treatment group. (Scale bar =50  $\mu$ m) (B) Expression of H2AX protein in HK-2 cells was analyzed by immunoblotting after 24 h of cisplatin and/or SQFZ treatment. (C) Quantitative results of B. Quantitative data represent the relative ratio to GAPDH. Values are shown as mean  $\pm$  SD in three independent experiments. \*  $P < 0.05$  as compared to Cisplatin alone.

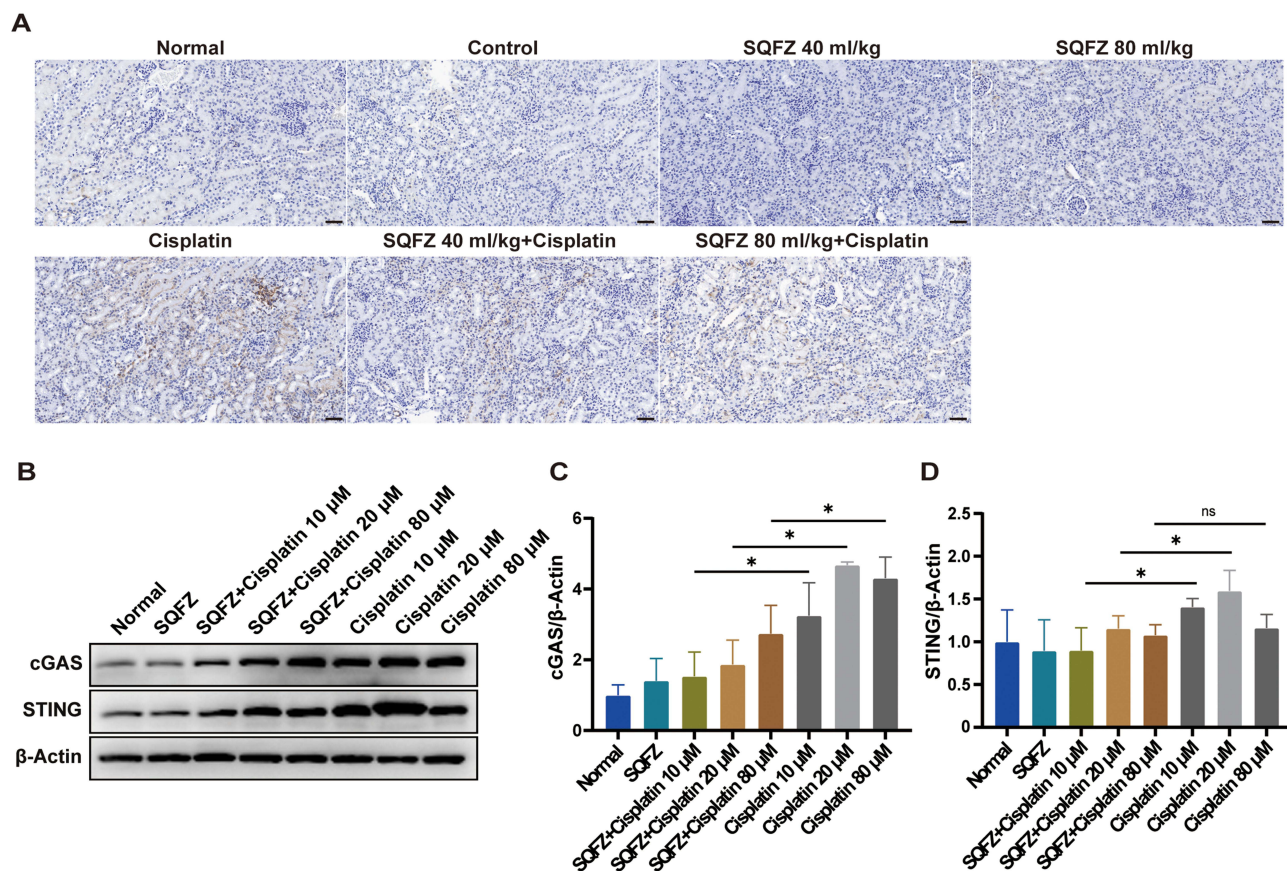


**Figure 6** Shenqi Fuzheng Injection inhibited the activation of cGAS/STING signaling pathway in cisplatin-treated mouse kidneys and HK-2 cells. **(A)** Immunohistochemical results of cGAS and STING in kidney tissues of mice in each treatment group. (Scale bar = 50 μm) **(B)** Expression of cGAS and STING protein in HK-2 cells was analyzed by immunoblotting after 24 h of cisplatin and/or SQFZ treatment. **(C and D)** Quantitative results of B. Quantitative data represent the relative ratio to β-Actin. Values are shown as mean ± SD in three independent experiments. \* $P < 0.05$  as compared to Cisplatin alone.

**Abbreviation** ns, not significant.

and STING protein expression levels were elevated in HK-2 cells subjected to cisplatin treatment for 24 h. In contrast, SQFZ plus cisplatin treatment had the opposite effects ( $P < 0.05$ ) (Figure 6B and C). The cGAS and STING protein expression levels did not significantly increase with cisplatin concentration. They were highest in response to 20 μM cisplatin.

## The protective effects of Shenqi Fuzheng Injection are associated with mitochondrial function in HK-2 cells

Mitochondrial homeostasis is vital to kidney function. Mitochondrial dysfunction is a key factor in the development of kidney injury.<sup>54,55</sup> Mitochondria undergo aerobic respiration to generate the ATP that is essential for driving multiple metabolic and physiological processes. Hence, mitochondrial function may be evaluated by measuring the ATP levels.<sup>56</sup> Here, the HK-2 cells treated with cisplatin for 24 h presented significant reductions in ATP compared to the untreated control. This effect was partially reversed by the combined SQFZ-cisplatin treatments. Moreover, SQFZ alone increased ATP expression relative to the untreated control ( $P < 0.05$ ) (Figure 7A). A JC-1 probe revealed that the HK-2 cells treated with cisplatin for 24 h presented with lower MMP and a higher proportion of JC-1 monomers than the untreated control (Figure 7B). The ratio of pro-apoptotic Bax to anti-apoptotic Bcl2 reflects the extent of mitochondria-mediated apoptosis.<sup>57</sup> Bax-mediated mitochondrial outer membrane permeabilization (MOMP) increased membrane permeability and, consequently, mtDNA effluxed into the cytosol.<sup>58</sup> A Western blot assay disclosed that the HK-2 cells subjected to cisplatin for 24 h exhibited higher percentages of Bax than the untreated control. However, the combined SQFZ-cisplatin treatment had the opposite effect (Figure 7C). The combined SQFZ-cisplatin treatment did not reverse the changes in the Bax/Bcl2 ratio caused by 80 μM cisplatin.

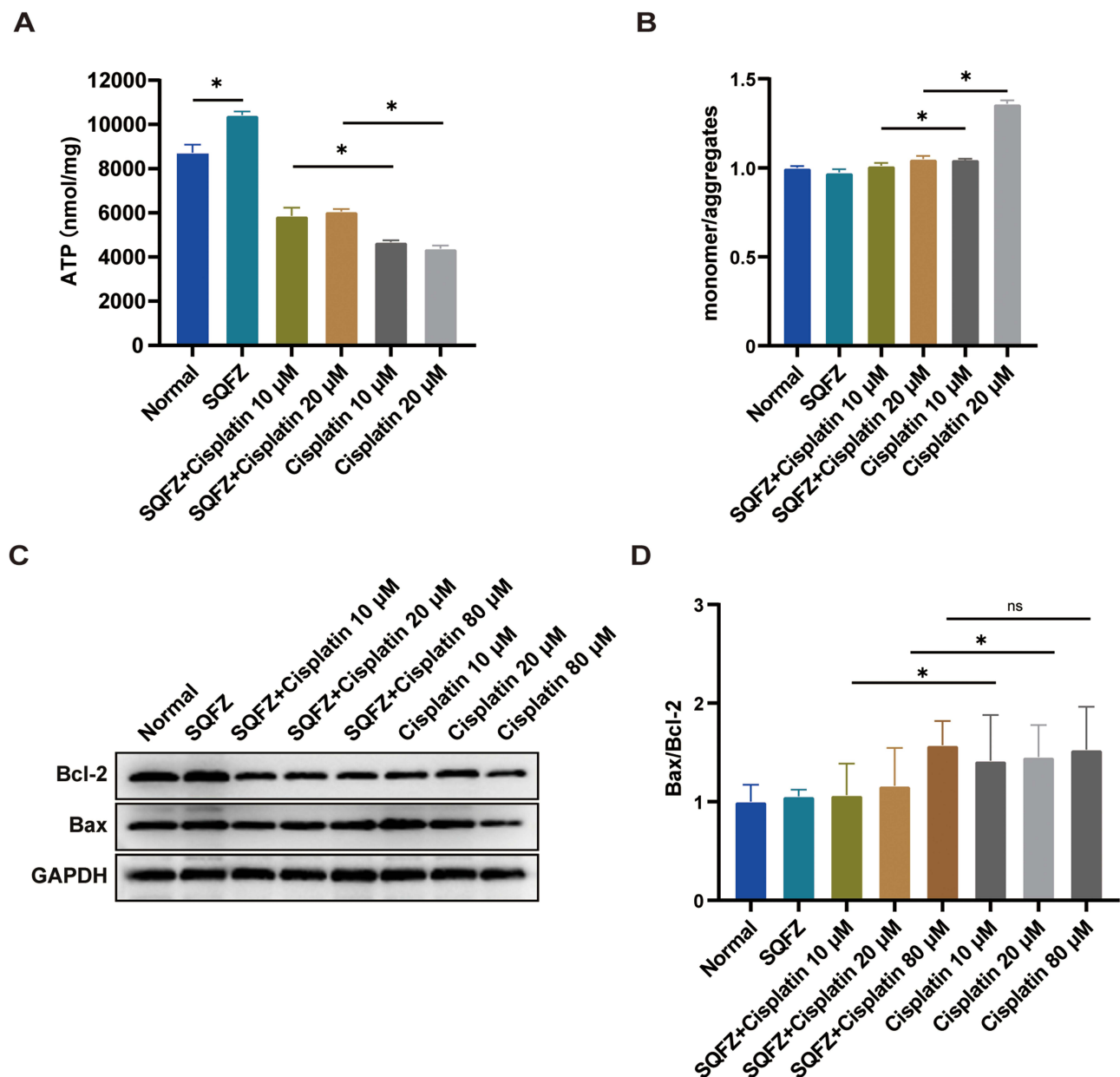


**Figure 7** The protective effect of Shenqi Fuzheng Injection on HK-2 cells is associated with mitochondrial function. (A-D) HK-2 cells were treated with cisplatin and SQFZ for 24 h. (A) Results of ATP level assay in HK-2 cells. (B) Monomer/aggregates values were used to represent JC-1 assay. (C) Expression of Bax and Bcl-2 protein in HK-2 cells was analyzed by immunoblotting. (D) Quantitative results of C. Quantitative data represent the relative ratio of Bax to Bcl-2. Values are shown as mean  $\pm$  SD in three independent experiments. \*  $P < 0.05$  as compared between the two groups.

**Abbreviation** ns, not significant.

## Shenqi Fuzheng Injection Ameliorates Cisplatin-Induced Tubular Inflammation Through STING

To address the molecular mechanism by which the STING pathway contributed to tubular inflammation in cisplatin-induced kidney injury treated with SQFZ, we evaluated the secretion of the inflammatory cytokines in serum and the effect of the STING pathway in immortalized HK-2 proximal tubular cells exposed to cisplatin alone or combined with SQFZ. We found that cisplatin-induced tubular damage was associated with an increase in cisplatin-induced expression of inflammatory molecules IL-6, IL-8, CCL5 and NO in serum (Figure 8A). Importantly, HK-2 cells knocked down the STING by small interfering RNA (siRNA) showed that the increased expression and secretion of IL-6 and IL-8, as well

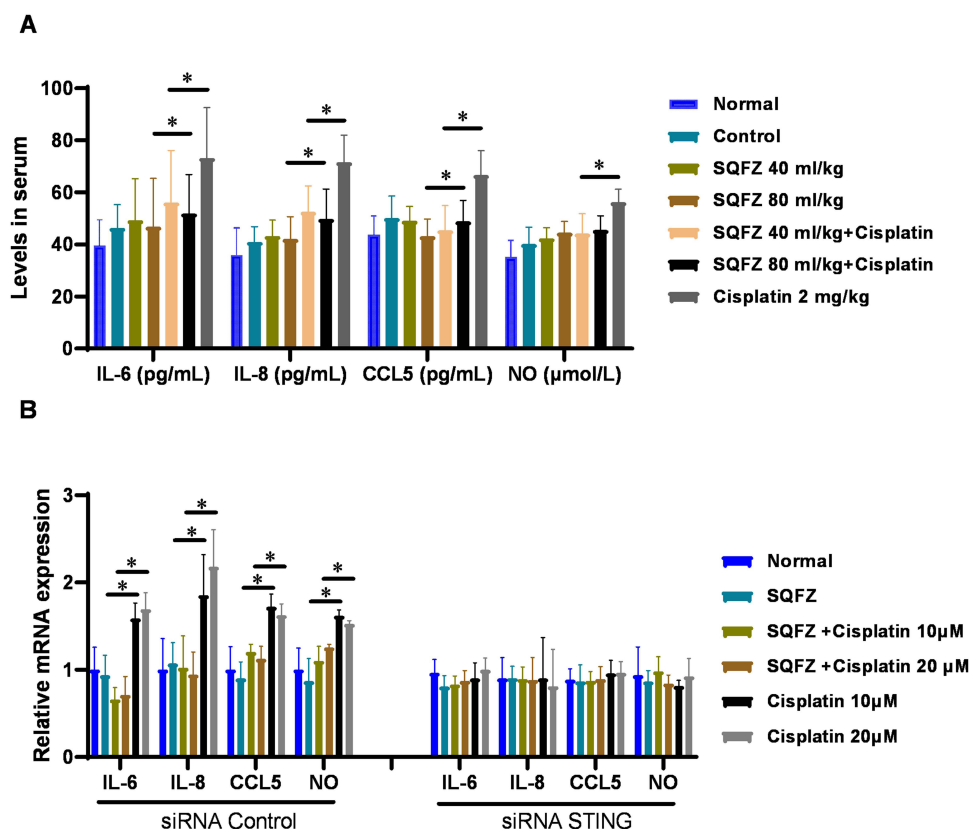


**Figure 8** Shenqi Fuzheng Injection ameliorates cisplatin-induced the secretion of the inflammatory cytokines through STING. **(A)** BALB/c mice inoculated with 4T1 cells in the fat pads were treated with daily intraperitoneal injections of saline or SQFZ 40, 80 mL/kg, cisplatin 2 mg/kg, SQFZ 40 mL/kg + cisplatin (injected every three days), and SQFZ 80 mL/kg + cisplatin (injected every three days) for 18 days. Levels of IL-6, IL-8, CCL5 and NO in serum were analyzed by ELISA assay ( $n = 6$  per group). **(B)** siRNA-mediated STING knockdown reversed the upregulation of IL-6, IL-8, CCL5, and NO in cisplatin-treated HK-2 cells in presence of SQFZ by quantitative real-time PCR. \*  $P < 0.05$  as compared to Cisplatin alone.

as other inflammation-related molecules CCL5 and NO by cisplatin, were markedly reversed by STING knockdown in the presence of SQFZ ( $P < 0.05$ ), as determined with quantitative real-time PCR (Figure 8B).

## Discussion

Kidney injury is a toxic effect of cisplatin and may negatively impact the quality of life and survival in cancer patients.<sup>59,60</sup> Kidney injury induced by cisplatin could be minimized by combining with Chinese herbs.<sup>61,62</sup> Here, we postulated that the traditional Chinese medicine (TCM) known as SQFZ could ameliorate cisplatin-induced kidney injury. Serum BUN and CRE, the secretion of inflammatory cytokines and pathological changes of kidney were observed to evaluate the kidney injury effect of SQFZ. We found that SQFZ enhanced the therapeutic efficacy of cisplatin, reduced the tumor size and alleviated cisplatin toxicity to a significantly greater extent than cisplatin alone (Figure 2A–C). Furthermore, SQFZ also protected HK-2 cells against cisplatin toxicity (Figure 2G and H). Due to individual differences in experimental mice, there are significant variations in tumor weight, which may be improved by increasing the number of experimental mice. These results suggested that SQFZ attenuated cisplatin-induced renal tubular epithelial cell apoptosis both in vivo and in vivo (Figure 4A–C).

Mitochondrial dysfunction played an integral role in the mechanism of cisplatin-induced kidney injury.<sup>63</sup> When mitochondria produced excessive intracellular ROS, they triggered oxidative stress, inflammatory response, and, by extension, kidney injury.<sup>64</sup> Cisplatin induced excessive ROS accumulation in renal tubular epithelial cells.<sup>65</sup> It also downregulated the vital antioxidant GSH.<sup>66</sup> We found that cisplatin increased the ROS levels in HK-2 cells and decreased the serum GSH levels in mice (Figure 3A and B). Hence, SQFZ could ameliorate cisplatin-induced mitochondrial dysfunction-related oxidative stress both in vivo and in vitro.

Mitochondrial dysfunction was also associated with decreases in ATP production and mitochondrial membrane potential (MMP).<sup>67,68</sup> Here, we empirically demonstrated that cisplatin lowered both ATP production and the MMP whereas SQFZ had the opposite effects (Figure 7A and B). In cisplatin-induced kidney injury, Bax-mediated MOMP increased membrane permeability and, consequently, mtDNA was effluxed.<sup>36</sup> In the present work, we observed that cisplatin upregulated Bax in the HK-2 cells whereas SQFZ plus cisplatin treatment downregulated it (Figure 7C and D). However, SQFZ failed to lower the proportion of Bax in the presence of 80  $\mu\text{M}$  cisplatin as this high dosage might have severely damaged the HK-2 cells. Decreased drug accumulation is an important mechanism of platinum resistance in clinic.<sup>11,69</sup> Low concentrations of platinum caused solid tumors (squamous cell carcinoma and non-small cell lung cancer ect.) to become chemoresistant while higher concentrations of platinum are effective.<sup>70,71</sup> In high-risk breast cancer patients, they are also treated with high doses of platinum.<sup>72</sup> Therefore, it is necessary to refine the cisplatin concentration in subsequent experiments to further determine the optimal concentration for combination therapy. The preceding findings suggested that SQFZ protected HK-2 cells against cisplatin-induced injury by preserving their mitochondrial function.

H2A.X is a DNA damage marker.<sup>53</sup> Here, we discovered that SQFZ lowered the cisplatin-induced H2A.X levels in both mouse kidney tissue and HK-2 cells (Figure 5A–C). These discoveries implied that SQFZ protected against cisplatin-induced DNA damage both in vitro and in vivo. Cytosolic dsDNA and mtDNA leakage activated the cGAS/STING signaling pathway<sup>73</sup> which, in turn, caused an inflammatory response and exacerbates kidney injury.<sup>35</sup> We observed that SQFZ significantly inhibited cisplatin-induced STING activation in vivo (Figure 6A). In vitro, SQFZ counteracted cGAS upregulation in response to cisplatin exposure (Figure 6B and C). SQFZ also opposed STING upregulation induced by low (10  $\mu\text{M}$  or 20  $\mu\text{M}$ ) cisplatin concentrations. However, SQFZ could not reverse STING upregulation induced by 80  $\mu\text{M}$  cisplatin (Figure 6B–D). Thus, cisplatin-induced kidney injury damaged mitochondria and caused cytosolic mtDNA leakage which activated the cGAS/STING signaling pathway.<sup>36</sup> Whereas SQFZ partially reversed Bax-induced mtDNA leakage, it could not effectively negate the toxic effects of high cisplatin concentrations. The results of this work indicated that SQFZ protected against cisplatin-induced kidney injury by mitigating mitochondrial DNA damage and inhibiting cGAS/STING signaling pathway activation. Moreover, STING knockout reversed the effect of SQFZ. SQFZ ameliorated cisplatin-induced tubular inflammation through STING pathway.

The present study showed that SQFZ improved cisplatin-induced renal injury by mitigating mitochondrial damage, mitochondrial DNA leakage, and cGAS/STING signaling pathway activation. This result provided a new option to ameliorate cisplatin-induced toxicity in clinic. SQFZ is an herbal compound with good antitumor efficacy and it improves the effectiveness and attenuates the toxicity of cisplatin.<sup>74</sup> Nevertheless, the mechanisms of SQFZ remained in tumor treatment to be clarified. In an earlier study, we investigated the mechanism by which SQFZ improved cisplatin resistance in breast cancer chemotherapy.<sup>50</sup> Here, we investigated the mode of action of SQFZ in ameliorating the kidney injury that could occur during the treatment of breast cancer with cisplatin. However, the pathways through which SQFZ acted on the mitochondrial and cGAS/STING signaling pathways and how it subsequently acted on the kidney need to be further explored. Combinations of SQFZ plus cisplatin have demonstrated promising therapeutic efficacy against breast cancer. The best dosage and interval of giving the combination of drugs also need to be further determined for better application to the clinic. It is also possible to try to explore what effects can be obtained by combining SQFZ with other chemotherapeutic agents. Future investigations will endeavor to elucidate the pharmacological mode of action of SQFZ as a co-treatment for various cancers by establishing other cancer models.

## Conclusions

The study found that Shenqi Fuzheng Injection (SQFZ) improved cisplatin-induced mitochondrial dysfunction and inhibited apoptosis in renal tubular epithelial cells by reducing mitochondrial oxidative stress, preventing mtDNA leakage, and increasing ATP levels and mitochondrial membrane potential (MMP). Additionally, SQFZ inhibited the cGAS/STING signaling pathway, which is associated with the inflammatory response in kidney injury. These findings suggested that SQFZ could protect the kidneys from cisplatin-induced damage by preventing apoptosis related to mitochondrial dysfunction and suppressing the cGAS/STING pathway. The study highlights SQFZ as a potential therapeutic option to reduce cisplatin's nephrotoxicity, though further research is needed to fully understand its mechanism, optimal dosing, and potential use with other chemotherapeutic agents (Figure 9).

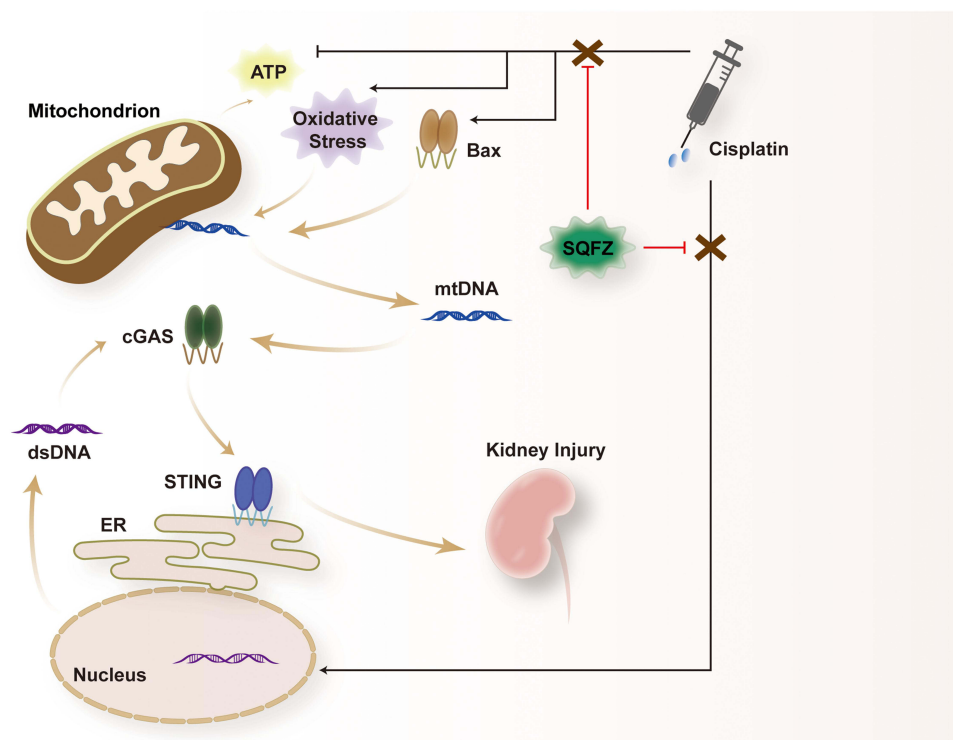


**Figure 9** SQZ was able to protect against cisplatin-induced renal injury by reducing oxidative stress, improving mitochondrial dysfunction, blocking mtDNA leakage, and inhibiting activation of the cGAS/STING pathway.

## Abbreviations

AKI, acute kidney injury; AMP, adenosine monophosphate; BUN, blood urea nitrogen; cAKI, Cisplatin-induced AKI; cGAS, cyclic guanosine monophosphate-adenosine monophosphate synthase; CRE, creatinine; DDR, DNA damage response; DMEM, Dulbecco's modified Eagle's medium; dsDNA, double-stranded DNA; FBS, fetal bovine serum; GMP, cyclic guanosine monophosphate; GSH glutathione; HE, hematoxylin-eosin staining; HK-2, renal tubular epithelial cells; IHC, immunohistochemistry; IP, intraperitoneally; MMP, mitochondrial membrane potential; MOMP, mitochondrial outer membrane permeabilization; mtDNA, Mitochondrial DNA; MTT, 3-(4,5-dimethylthiazol-2-yl)-2,5-diphenyl-2H-tetrazolium bromide; PI, propidium iodide; PI3K, phosphoinositide 3-kinase; QoL, quality of life; ROS reactive oxygen species; SOD, superoxide dismutase; SQFZ, Shenqi Fuzheng Injection; STING, stimulator of interferon genes; TCM, traditional Chinese medicine; TUNEL, terminal deoxynucleotidyl transferase dUTP nick end labeling; 4T1, Mouse breast cancer cells.

## Data Sharing Statement

The data included in this investigation are available from the corresponding author. The authors confirm that the data supporting the findings of this study are available within the article.

## Ethical Statement

All animal studies (including the mouse euthanasia procedure) were done in compliance with the regulations and guidelines of the animal ethics committee of Shanghai Traditional Chinese Medicine under Approval No. PZSHUTCM220919006.

## Acknowledgments

This work was financially supported by Shanghai Traditional Chinese Medicine High-level Talents Leading Program Project, Science and Technology Commission of Shanghai Municipality Project (22ZR1446900 and 21ZR1447800),

Peak Disciplines (Type IV) of Institutions of Higher Learning in Shanghai and the Science and Technology Development Project of Shanghai University of Traditional Chinese Medicine (23KFL020). Thanks to Jing Wang and Weihong Zhang for their contributions to this article.

## Author Contributions

All authors made a significant contribution to the work reported, whether that is in the conception, study design, execution, acquisition of data, analysis and interpretation, or in all these areas; took part in drafting, revising or critically reviewing the article; gave final approval of the version to be published; have agreed on the journal to which the article has been submitted; and agree to be accountable for all aspects of the work.

## Disclosure

The authors declare that the research was conducted in the absence of any commercial or financial relationships that could be construed as a potential conflict of interest.

## References

1. Miller KD, Nogueira L, Devasia T, et al. Cancer treatment and survivorship statistics, 2022. *CA Cancer J Clin.* 2022;72(5):409–436. doi:10.3322/caac.21731
2. Zheng RS, Zhang SW, Sun KX, et al. [Cancer statistics in China, 2016]. *Zhonghua Zhong Liu Za Zhi.* 2023;45(3):212–00647. doi:10.3760/cma.j.cn112152-20220922-00647
3. Sathishkumar K, Chaturvedi M, Das P, Stephen S, Mathur P. Cancer incidence estimates for 2022 & projection for 2025: Result from National Cancer Registry Programme, India. *Indian J Med Res.* 2022;156(4):598–607. doi:10.4103/ijmr.ijmr\_1821\_22
4. Tufail M, Wu C. Cancer statistics in Pakistan from 1994 to 2021: data from cancer registry. *JCO Clin Cancer Inform.* 2023;7(7):e2200142. doi:10.1200/cci.22.00142
5. Siegel RL, Miller KD, Wagle NS, Jemal A. Cancer statistics, 2023. *CA Cancer J Clin.* 2023;73(1):17–48. doi:10.3322/caac.21763
6. Bray F, Laversanne M, Sung H, et al. Global cancer statistics 2022: GLOBOCAN estimates of incidence and mortality worldwide for 36 cancers in 185 countries. *CA Cancer J Clin.* 2024;74:229–263. doi:10.3322/caac.21834
7. Fakhri N, Chad MA, Lahkim M, et al. Risk factors for breast cancer in women: an update review. *Med Oncol.* 2022;39:197. doi:10.1007/s12032-022-01804-x
8. Peairs KS, Choi Y, Stewart RW, Sateia HF. Screening for breast cancer. *Semin Oncol.* 2017;44:60–72. doi:10.1053/j.seminoncol.2017.02.004
9. Davey MG, Lowery AJ, Miller N, Kerin MJ. MicroRNA expression profiles and breast cancer chemotherapy. *Int J Mol Sci.* 2021;22:10812. doi:10.3390/ijms221910812
10. Siegel RL, Miller KD, Fuchs HE, Jemal A. Cancer statistics, 2022. *CA Cancer J Clin.* 2022;72:7–33. doi:10.3322/caac.21708
11. Ghosh S. Cisplatin: the first metal based anticancer drug. *Bioorg Chem.* 2019;88:102925. doi:10.1016/j.bioorg.2019.102925
12. Rodler E, Sharma P, Barlow WE, et al. Cisplatin with veliparib or placebo in metastatic triple-negative breast cancer and BRCA mutation-associated breast cancer (S1416): a randomised, double-blind, placebo-controlled, Phase 2 trial. *Lancet Oncol.* 2023;24:162–174. doi:10.1016/s1470-2045(22)00739-2
13. Tang C, Livingston MJ, Safirstein R, Dong Z. Cisplatin nephrotoxicity: new insights and therapeutic implications. *Nat Rev Nephrol.* 2023;19:53–72. doi:10.1038/s41581-022-00631-7
14. Zhang X, Trendowski MR, Wilkinson E, et al. Pharmacogenomics of cisplatin-induced neurotoxicities: hearing loss, tinnitus, and peripheral sensory neuropathy. *Cancer Med.* 2022;11:2801–2816. doi:10.1002/cam4.4644
15. Kros CJ, Steyger PS. Aminoglycoside- and cisplatin-induced ototoxicity: mechanisms and otoprotective strategies. *Cold Spring Harb Perspect Med.* 2019;9:a033548. doi:10.1101/cshperspect.a033548
16. Huang TH, Chiu YH, Chan YL, et al. Antrodia cinnamomea alleviates cisplatin-induced hepatotoxicity and enhances chemo-sensitivity of line-1 lung carcinoma xenografted in BALB/cByJ mice. *Oncotarget.* 2015;6:25741–25754. doi:10.18632/oncotarget.4348
17. Xing JJ, Hou JG, Liu Y, et al. Supplementation of saponins from leaves of panax quinquefolius mitigates cisplatin-evoked cardiotoxicity via inhibiting oxidative stress-associated inflammation and apoptosis in mice. *Antioxidants.* 2019;8:347. doi:10.3390/antiox8090347
18. Yin Q, Zhao YJ, Ni WJ, et al. MiR-155 deficiency protects renal tubular epithelial cells from telomeric and genomic DNA damage in cisplatin-induced acute kidney injury. *Theranostics.* 2022;12:4753–4766. doi:10.7150/thno.72456
19. Latcha S, Jaimes EA, Patil S, Glezerman IG, Mehta S, Flombaum CD. Long-term renal outcomes after cisplatin treatment. *Clin J Am Soc Nephrol.* 2016;11:1173–1179. doi:10.2215/cjn.08070715
20. Xu Y, Ma H, Shao J, et al. A role for tubular necroptosis in cisplatin-induced AKI. *J Am Soc Nephrol.* 2015;26:2647–2658. doi:10.1681/asn.2014080741
21. Tang C, Cai J, Yin XM, Weinberg JM, Venkatachalam MA, Dong Z. Mitochondrial quality control in kidney injury and repair. *Nat Rev Nephrol.* 2021;17:299–318. doi:10.1038/s41581-020-00369-0
22. Wei MC, Zong WX, Cheng EH, et al. Proapoptotic BAX and BAK: a requisite gateway to mitochondrial dysfunction and death. *Science.* 2001;292:727–730. doi:10.1126/science.1059108
23. Jiang M, Wang CY, Huang S, Yang T, Dong Z. Cisplatin-induced apoptosis in p53-deficient renal cells via the intrinsic mitochondrial pathway. *Am J Physiol Renal Physiol.* 2009;296:F983–993. doi:10.1152/ajprenal.90579.2008
24. Li T, Baochen Z, Yue W, et al. Network pharmacology-based identification of pharmacological mechanism of SQFZ injection in combination with docetaxel on lung cancer. *Sci Rep.* 2019;9:4533. doi:10.1038/s41598-019-40954-3

25. Alanezi AA, Almuqati AF, Alfwaaires MA, et al. Taxifolin prevents cisplatin nephrotoxicity by modulating Nrf2/HO-1 pathway and mitigating oxidative stress and inflammation in mice. *Pharmaceuti*. 2022;15:1310. doi:10.3390/ph15111310
26. Bhargava P, Schnellmann RG. Mitochondrial energetics in the kidney. *Nat Rev Nephrol*. 2017;13:629–646. doi:10.1038/nrneph.2017.107
27. Airik M, Arbore H, Childs E, et al. Mitochondrial ROS triggers kidney pathogenesis in fan1-deficient kidneys. *Antioxidants (Basel)*. 2023;12:900. doi:10.3390/antiox12040900
28. Hu J, Gu W, Ma N, et al. Leonurine alleviates ferroptosis in cisplatin-induced acute kidney injury by activating the Nrf2 signalling pathway. *Br J Pharmacol*. 2022;179:3991–4009. doi:10.1111/bph.15834
29. Hasegawa K, Wakino S, Yoshioka K, et al. Kidney-specific overexpression of Sirt1 protects against acute kidney injury by retaining peroxisome function. *J Biol Chem*. 2010;285:13045–13056. doi:10.1074/jbc.M109.067728
30. Ratliff BB, Abdulmahdi W, Pawar R, Wolin MS. Oxidant Mechanisms in Renal Injury and Disease. *Antioxid Redox Signal*. 2016;25:119–146. doi:10.1089/ars.2016.6665
31. Basu A, Krishnamurthy S. Cellular responses to cisplatin-induced DNA damage. *J Nucleic Acids*. 2010;(2010):201367. doi:10.4061/2010/201367
32. Zhao M, Wang Y, Li L, et al. Mitochondrial ROS promote mitochondrial dysfunction and inflammation in ischemic acute kidney injury by disrupting TFAM-mediated mtDNA maintenance. *Theranostics*. 2021;11:1845–1863. doi:10.7150/thno.50905
33. Hu Y, Yang C, Amorim T, et al. Cisplatin-mediated upregulation of APE2 binding to MYH9 provokes mitochondrial fragmentation and acute kidney injury. *Cancer Res*. 2021;81:713–723. doi:10.1158/0008-5472.Can-20-1010
34. Lu J, Zhang Y, Dong H, et al. New mechanism of nephrotoxicity of triptolide: oxidative stress promotes cGAS-STING signaling pathway. *Free Radic Biol Med*. 2022;188:26–34. doi:10.1016/j.freeradbiomed.2022.06.009
35. Gao X, Wang J, Wang Y, et al. Fucoidan-ferulic acid nanoparticles alleviate cisplatin-induced acute kidney injury by inhibiting the cGAS-STING pathway. *Int J Biol Macromol*. 2022;223:1083–1093. doi:10.1016/j.ijbiomac.2022.11.062
36. Maekawa H, Inoue T, Ouchi H, et al. Mitochondrial damage causes inflammation via cGAS-STING signaling in acute kidney injury. *Cell Rep*. 2019;29:1261–1273.e1266. doi:10.1016/j.celrep.2019.09.050
37. Harapas CR, Idiattullina E, Al-Azab M, et al. Organellar homeostasis and innate immune sensing. *Nat Rev Immunol*. 2022;22:535–549. doi:10.1038/s41577-022-00682-8
38. Heilig R, Lee J, Tait SWG. Mitochondrial DNA in cell death and inflammation. *Biochem Soc Trans*. 2023;51:457–472. doi:10.1042/bst20221525
39. Chen Z, Meng CL, Wang XL, et al. Ultrasensitive DNA Origami Plasmon Sensor for Accurate Detection in Circulating Tumor DNAs. *Laser Photonics Rev*. 2024. doi:10.1002/lpor.202400035
40. Xu J, Li X, Lv L, et al. The role of Shenqi Fuzheng injection as adjuvant therapy for breast cancer: an overview of systematic reviews and meta-analyses. *BMC Complement Med Ther*. 2024;24:33. doi:10.1186/s12906-023-04274-4
41. Wu X, Liu Y, Zhang Z, et al. Authentication of Shenqi Fuzheng Injection via UPLC-coupled ion mobility-mass spectrometry and chemometrics with Kendrick mass defect filter data mining. *Molecules*. 2022;27:4734. doi:10.3390/molecules27154734
42. Chen J, Wei X, Zhang Q, et al. The traditional Chinese medicines treat chronic heart failure and their main bioactive constituents and mechanisms. *Acta Pharm Sin B*. 2023;13:1919–1955. doi:10.1016/j.apsb.2023.02.005
43. Ma Y, Qi Y, Zhou Z, et al. Shenqi Fuzheng injection modulates tumor fatty acid metabolism to downregulate MDSCs infiltration, enhancing PD-L1 antibody inhibition of intracranial growth in Melanoma. *Phytomedicine*. 2024;122:155171. doi:10.1016/j.phymed.2023.155171
44. Yang M, Zhu SJ, Shen C, et al. Clinical application of Chinese herbal injection for cancer care: evidence-mapping of the systematic reviews, meta-analyses, and randomized controlled trials. *Front Pharmacol*. 2021;12:666368. doi:10.3389/fphar.2021.666368
45. Meng FX, Yang X, Li ML. Shenqi Fuzheng Injection () Combined with Chemotherapy for Acute Leukemia: a Meta-Analysis. *Chin J Integr Med*. 2022;28:81–87. doi:10.1007/s11655-020-3264-7
46. Dong J, Su SY, Wang MY, Zhan Z. Shenqi fuzheng, an injection concocted from Chinese medicinal herbs, combined with platinum-based chemotherapy for advanced non-small cell lung cancer: a systematic review. *J Exp Clin Cancer Res*. 2010;29:137. doi:10.1186/1756-9966-29-137
47. Zhu G, Zhang B, Jiang F, Zhao L, Liu F. ShenQi FuZheng Injection ameliorates fatigue-like behavior in mouse models of cancer-related fatigue. *Biomed Pharmacother*. 2019;111:1376–1382. doi:10.1016/j.biopha.2019.01.042
48. Gao W, Zhang K. Network meta-analysis of 8 types of traditional Chinese medicine injection combined with chemotherapy in colorectal cancer treatment. *J Cancer Res Clin Oncol*. 2023;149:9823–9838. doi:10.1007/s00432-023-04892-y
49. Bo Y, Li HS, Qi YC, Lu MY. Clinical study on treatment of mammary cancer by shenqi fuzheng injection in cooperation with chemotherapy. *Chin J Integr Med*. 2007;13:37–40. doi:10.1007/s11655-007-0037-5
50. Yan B, Shi R, Lu YY, Fang DD, Ye MN, Zhou QM. Shenqi Fuzheng injection reverses M2 macrophage-mediated cisplatin resistance through the PI3K pathway in breast cancer. *PLoS One*. 2023;18:e0279752. doi:10.1371/journal.pone.0279752
51. Su L, Zhang J, Gomez H, Kellum JA, Peng Z. Mitochondria ROS and mitophagy in acute kidney injury. *Autophagy*. 2023;19:401–414. doi:10.1080/15548627.2022.2084862
52. Niu B, Liao K, Zhou Y, et al. Application of glutathione depletion in cancer therapy: enhanced ROS-based therapy, ferroptosis, and chemotherapy. *Biomaterials*. 2021;277:121110. doi:10.1016/j.biomaterials.2021.121110
53. Sharma A, Singh K, Almasan A. Histone H2AX phosphorylation: a marker for DNA damage. *Methods Mol Biol*. 2012;920:613–626. doi:10.1007/978-1-61779-998-3\_40
54. Hall AM, Schuh CD. Mitochondria as therapeutic targets in acute kidney injury. *Curr Opin Nephrol Hypertens*. 2016;25:355–362. doi:10.1097/mnh.0000000000000228
55. Zhu L, Yuan Y, Yuan L, et al. Activation of TFEB-mediated autophagy by trehalose attenuates mitochondrial dysfunction in cisplatin-induced acute kidney injury. *Theranostics*. 2020;10:5829–5844. doi:10.7150/thno.44051
56. Zhang X, Agborbesong E, Li X. The role of mitochondria in acute kidney injury and chronic kidney disease and its therapeutic potential. *Int J Mol Sci*. 2021;22:11253. doi:10.3390/ijms222011253
57. Peña-Blanco A, García-Sáez AJ. Bax, bak and beyond - mitochondrial performance in apoptosis. *Febs j*. 2018;285:416–431. doi:10.1111/febs.14186
58. McArthur K, Whitehead LW, Heddleston JM, et al. Bak/bax macropores facilitate mitochondrial herniation and mtDNA efflux during apoptosis. *Science*. 2018;359:eaao6047. doi:10.1126/science.aao6047

59. McCulloch M, See C, Shu XJ, et al. Astragalus-based Chinese herbs and platinum-based chemotherapy for advanced non-small-cell lung cancer: meta-analysis of randomized trials. *J Clin Oncol*. 2006;24:419–430. doi:10.1200/jco.2005.03.6392
60. Mapuskar KA, Vasquez Martinez G, Pulliam CF, et al. Avasopasem manganese (GC4419) protects against cisplatin-induced chronic kidney disease: an exploratory analysis of renal metrics from a randomized phase 2b clinical trial in head and neck cancer patients. *Redox Biol*. 2023;60:102599. doi:10.1016/j.redox.2022.102599
61. Ju SM, Kim MS, Jo YS, et al. Licorice and its active compound glycyrrhizic acid ameliorates cisplatin-induced nephrotoxicity through inactivation of p53 by scavenging ros and overexpression of p21 in human renal proximal tubular epithelial cells. *Eur Rev Med Pharmacol Sci*. 2017;21:890–899.
62. Jin X, He R, Liu J, et al. An herbal formulation “ShenshuaiFu Granule” alleviates cisplatin-induced nephrotoxicity by suppressing inflammation and apoptosis through inhibition of the TLR4/MyD88/NF-κB pathway. *J Ethnopharmacol*. 2023;306:116168. doi:10.1016/j.jep.2023.116168
63. Yu X, Meng X, Xu M, et al. Celastrol ameliorates cisplatin nephrotoxicity by inhibiting NF-κB and improving mitochondrial function. *EBioMedicine*. 2018;36:266–280. doi:10.1016/j.ebiom.2018.09.031
64. Ichinomiya M, Shimada A, Ohta N, et al. Demonstration of mitochondrial damage and mitophagy in cisplatin-mediated nephrotoxicity. *Tohoku J Exp Med*. 2018;246:1–8. doi:10.1620/tjem.246.1
65. Mapuskar KA, Steinbach EJ, Zaher A, et al. Mitochondrial superoxide dismutase in cisplatin-induced kidney injury. *Antioxidants (Basel)*. 2021;10:1329. doi:10.3390/antiox10091329
66. Dong XQ, Chu LK, Cao X, et al. Glutathione metabolism rewiring protects renal tubule cells against cisplatin-induced apoptosis and ferroptosis. *Redox Rep*. 2023;28:2152607. doi:10.1080/13510002.2022.2152607
67. Burke PJ. Mitochondria, bioenergetics and apoptosis in cancer. *Trends Cancer*. 2017;3:857–870. doi:10.1016/j.trecan.2017.10.006
68. Perelman A, Wachtel C, Cohen M, Haupt S, Shapiro H, Tzur A. JC-1: alternative excitation wavelengths facilitate mitochondrial membrane potential cytometry. *Cell Death Dis*. 2012;3:e430. doi:10.1038/cddis.2012.171
69. Fu R, Zhao B, Chen M, et al. Moving beyond cisplatin resistance: mechanisms, challenges, and prospects for overcoming recurrence in clinical cancer therapy. *Med Oncol*. 2023;41:9. doi:10.1007/s12032-023-02237-w
70. Kim ES, Lee JJ, He G, et al. Tissue platinum concentration and tumor response in non-small-cell lung cancer. *J Clin Oncol*. 2012;30:3345–3352. doi:10.1200/jco.2011.40.8120
71. Kilari D, Guancial E, Kim ES. Role of copper transporters in platinum resistance. *World J Clin Oncol*. 2016;7:106–113. doi:10.5306/wjco.v7.i1.106
72. Hempel P, Müllert P, Oruzio D, et al. Combination of high-dose chemotherapy and monoclonal antibody in breast-cancer patients: a pilot trial to monitor treatment effects on disseminated tumor cells. *Cytotherapy*. 2000;2:287–295. doi:10.1080/146532400539224
73. Zhou J, Ventura CJ, Fang RH, Zhang L. Nanodelivery of STING agonists against cancer and infectious diseases. *Mol Aspects Med*. 2022;83:101007. doi:10.1016/j.mam.2021.101007
74. Xiong Y, Zhao Q, Gu L, et al. Shenqi fuzheng injection reverses cisplatin resistance through mitofusin-2-mediated cell cycle arrest and apoptosis in A549/DDP cells. *Evid Base Compl Alternat Med*. 2018;2018:8258246. doi:10.1155/2018/8258246

## Breast Cancer: Targets and Therapy

Dovepress

### Publish your work in this journal

Breast Cancer - Targets and Therapy is an international, peer-reviewed open access journal focusing on breast cancer research, identification of therapeutic targets and the optimal use of preventative and integrated treatment interventions to achieve improved outcomes, enhanced survival and quality of life for the cancer patient. The manuscript management system is completely online and includes a very quick and fair peer-review system, which is all easy to use. Visit <http://www.dovepress.com/testimonials.php> to read real quotes from published authors.

Submit your manuscript here: <https://www.dovepress.com/breast-cancer—targets-and-therapy-journal>